Supplementary Information: An equilibrium rotator glass-forming phase for long-ranged repulsive colloidal rods

Thijs Herman Besseling[1,2,*,†], Berend van der Meer[1,3], Bing Liu[1,4], Laura Filion[1], Arnout Imhof[1], Alfons van Blaaderen[1,*,‡]

[1] *Soft Condensed Matter and Biophysics, Debye Institute for Nanomaterials Science, Utrecht University, Princetonplein 5, 3584 CC Utrecht, The Netherlands*

[2] *Current affiliation: Imec at Holst Centre, High Tech Campus 31, 5656 AE Eindhoven, The Netherlands*

[3] *Current affiliation: Physical Chemistry and Soft Matter, Wageningen University and Research, Stippeneng 4, 6708 WE Wageningen, The Netherlands*

[4] *Current affiliation: Beijing National Laboratory for Molecular Sciences, Institute of Chemistry, Chinese Academy of Sciences 100190 Beijing, China*

[*] *Corresponding authors*

[†] *t.h.besseling@uu.nl*

[‡] *a.vanblaaderen@uu.nl*

(Dated: February 20, 2026)

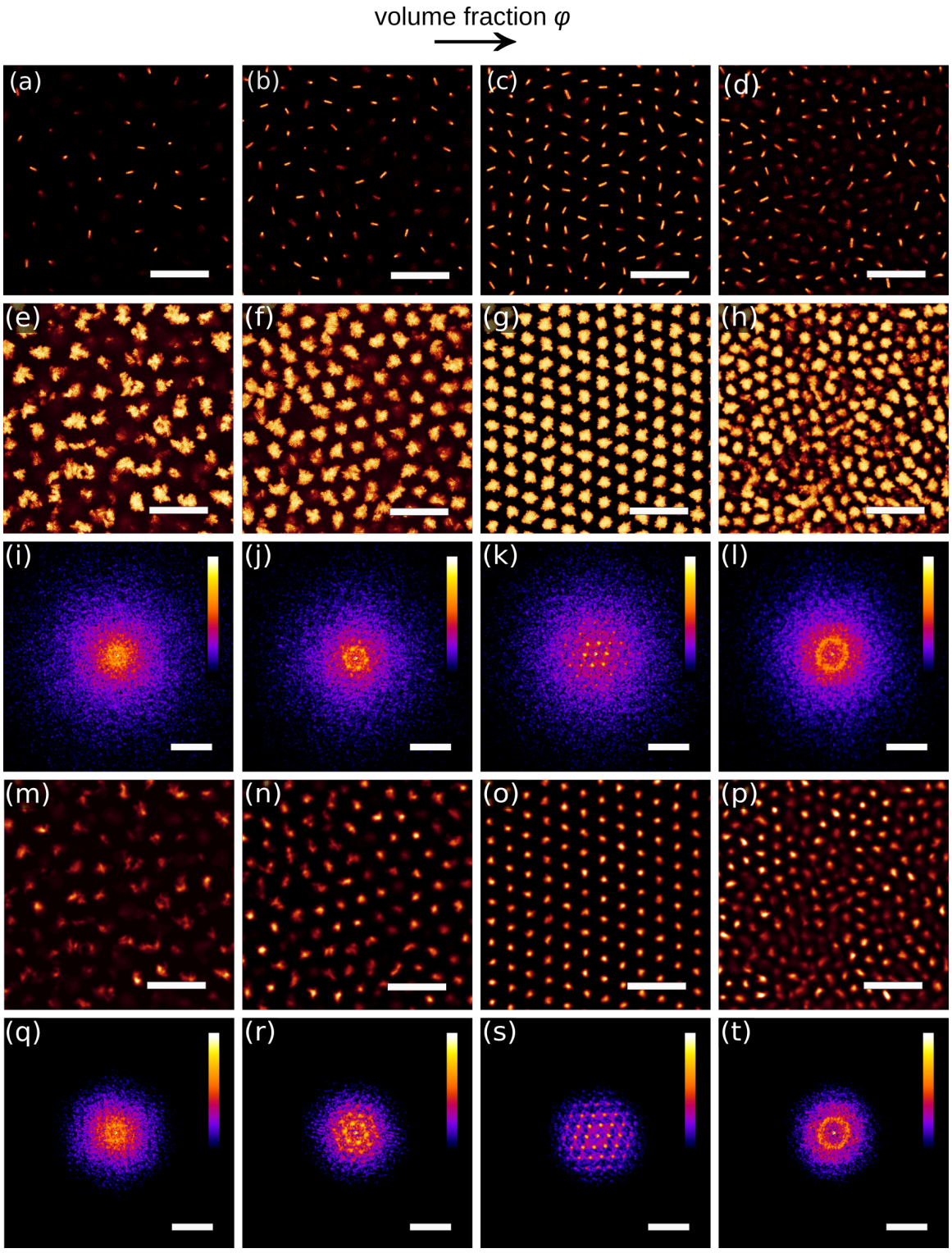

Supplementary FIG. 1: **Equilibrium phase transitions from a fluid to a glassy rotator phase**. (a-d) For fixed screening length ($\kappa l = 0.8$) but increasing volume fraction ϕ, particles form respectively a (dense) fluid phase (a), a plastic crystal phase (b) a denser plastic crystal phase (c) and a rotator glassy phase (d). (e-h) Maximum projection of 500 confocal microscopy images, representing a time window of 163 τ_t^0. (i-l) 2D FFTs from the images in (e-h). (m-p) Average intensity of the same 500 confocal microscopy images, representing the same time window of 163 τ_t^0. (q-t) 2D FFTs from the images in (m-p). All scale bars of real-space images are 15 μm, all scale bars of FFTs are 5 μm^{-1}. The FFTs show the logarithm of the intensity and a Hamming window was applied to avoid artefacts from the edges of the images.

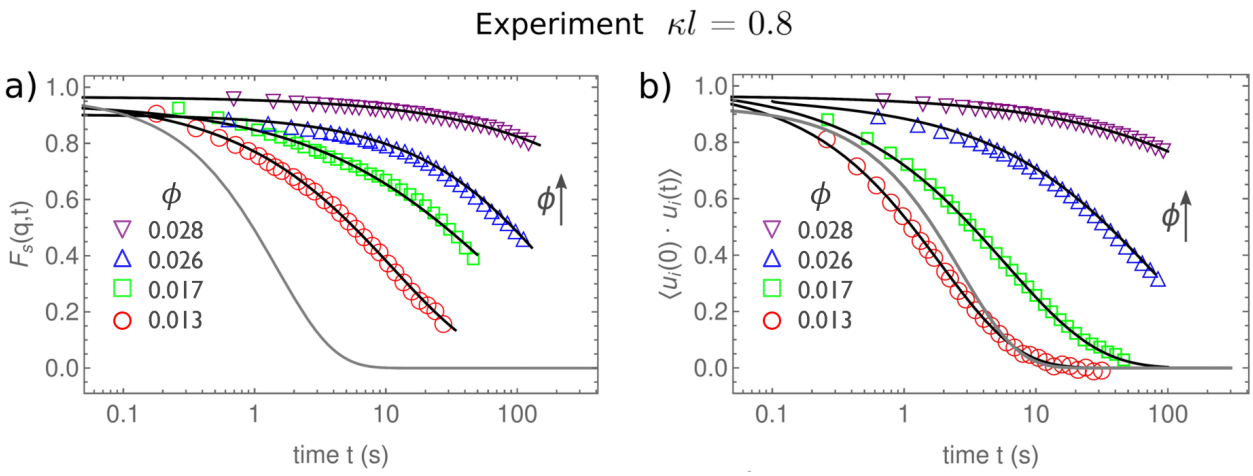

Supplementary FIG. 2: **Self-correlation functions for increasing volume fractions ϕ, obtained from 3D confocal microscopy image stacks.** (a) Self intermediate scattering function $F_s(q,t)$. (b) Orientation auto-correlation function $C(t)$. The grey continuous lines in a,b are theoretical prediction for rod-like particles at infinite dilution.

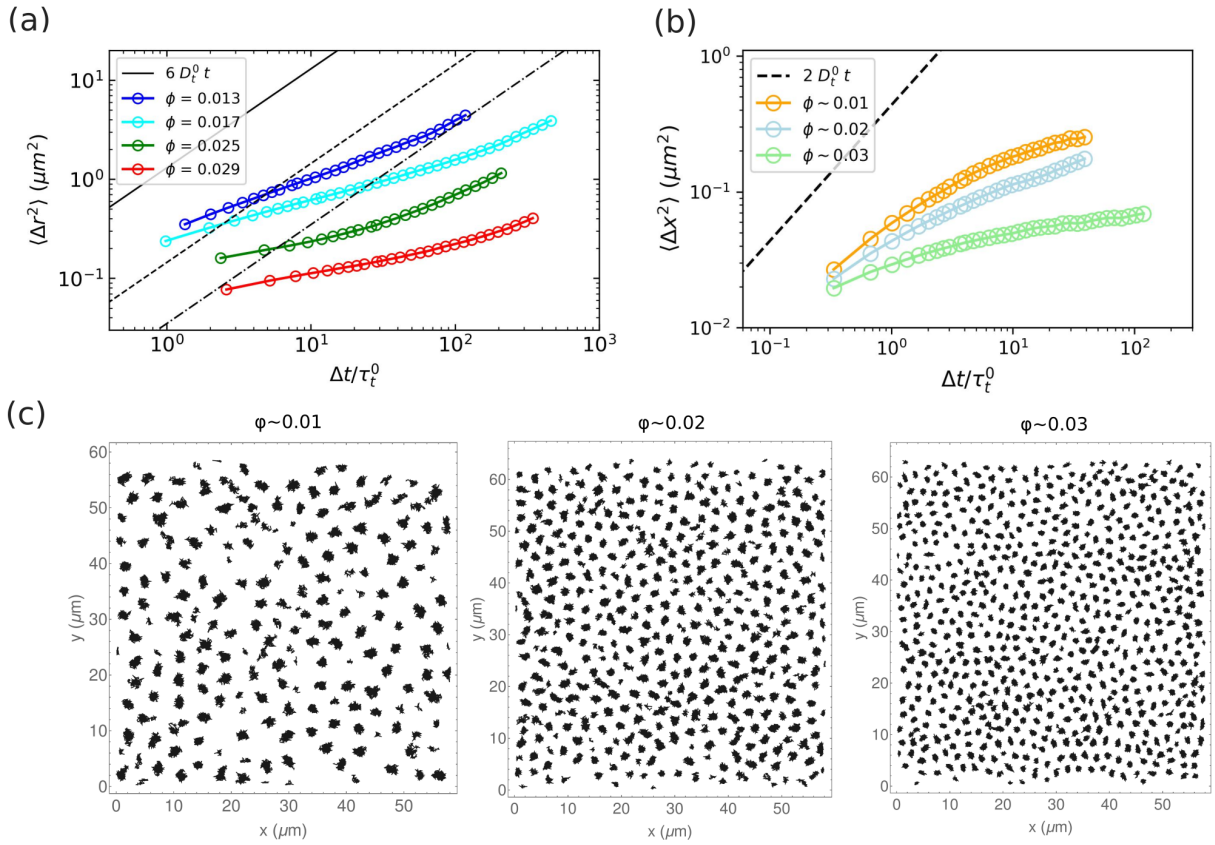

Supplementary FIG. 3: **Slowdown of translational motion in experimental system.** (a) Mean squared displacement $\langle \Delta r^2(t) \rangle$ obtained from 3D confocal microscopy image stacks, from increasing volume fraction ϕ. Black dashed lines indicate the regime were the long-term translational dynamics are diffusive again, i.e. $\langle \Delta r^2(t) \rangle \sim t$. (b) Mean squared displacement in the x-direction $\langle \Delta x^2(t) \rangle$, obtained from 2D confocal microscopy image stacks. (c) Particle trajectories of the samples plotted in (b).

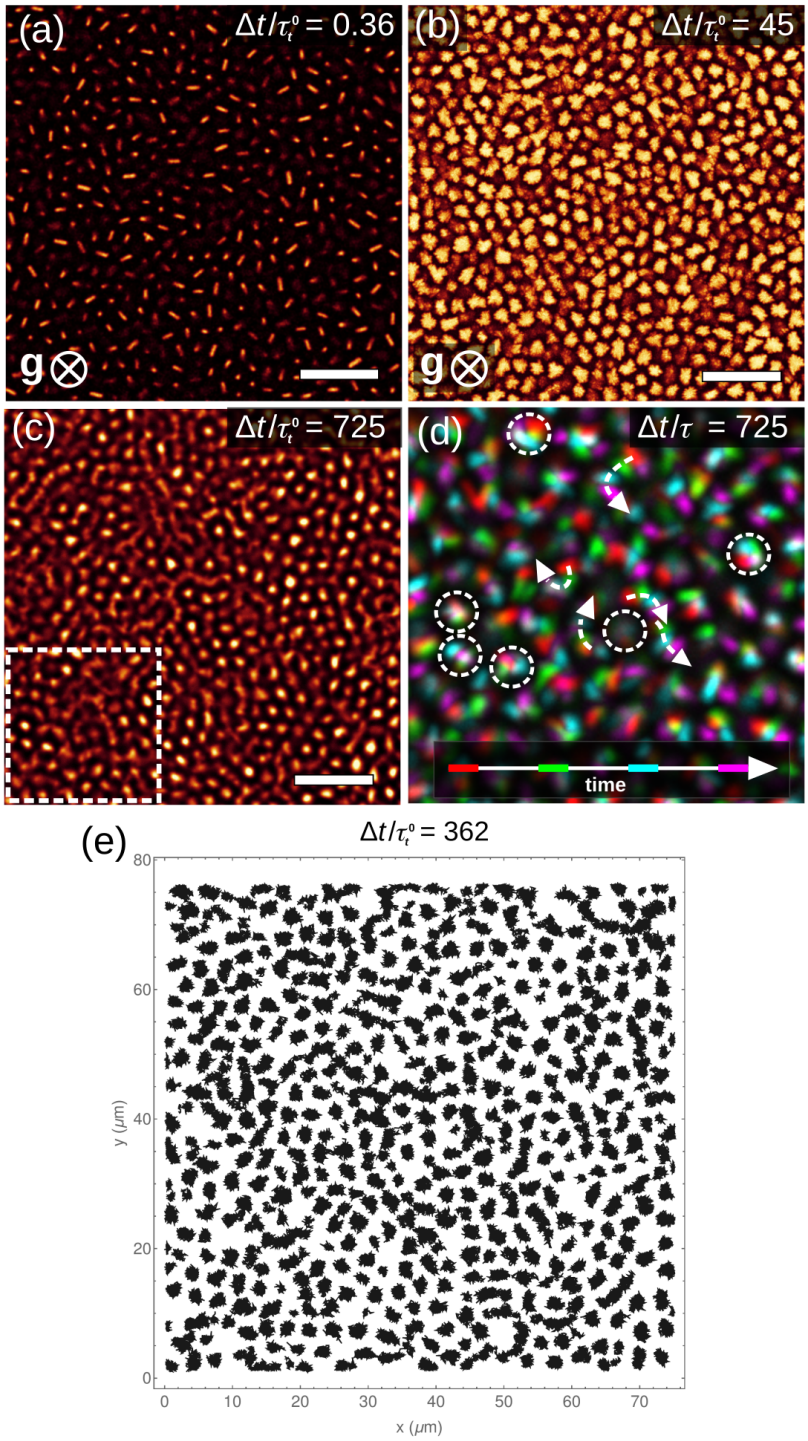

Supplementary FIG. 4: **Plastic glassy phase of long-ranged repulsive rods.** The volume fraction $\phi \sim 0.02$. The rotational relaxation time at infinite dilution is $\tau_R^0 = 2.5$ s and the time for the rod to diffuse over its own diameter at infinite dilution is $\tau_t^0 = 0.26$ s. (a) A single confocal microscopy snapshot shows the absence of long-ranged positional order. (b) A maximum projection of 125 individual images, representing a time window of 45 τ_t^0, shows that although there was significant rotational motion, the rods were positionally caged during this time interval. (c) An average of 2000 frames, representing a time window of 725 τ_t^0, shows that there were spatially heterogeneous rearrangements during this time interval. (d) Close-up of the region indicated in (c) with the (white) dashed line. The colours correspond to averages over time-intervals indicated in the figure. The dotted circles indicate particles with low mobility, whereas the dashed arrows indicate particles with high mobility. (e) 2D plot of the particle center-of-mass trajectories clearly shows dynamical heterogeneities. All scale bars are 15 μm.

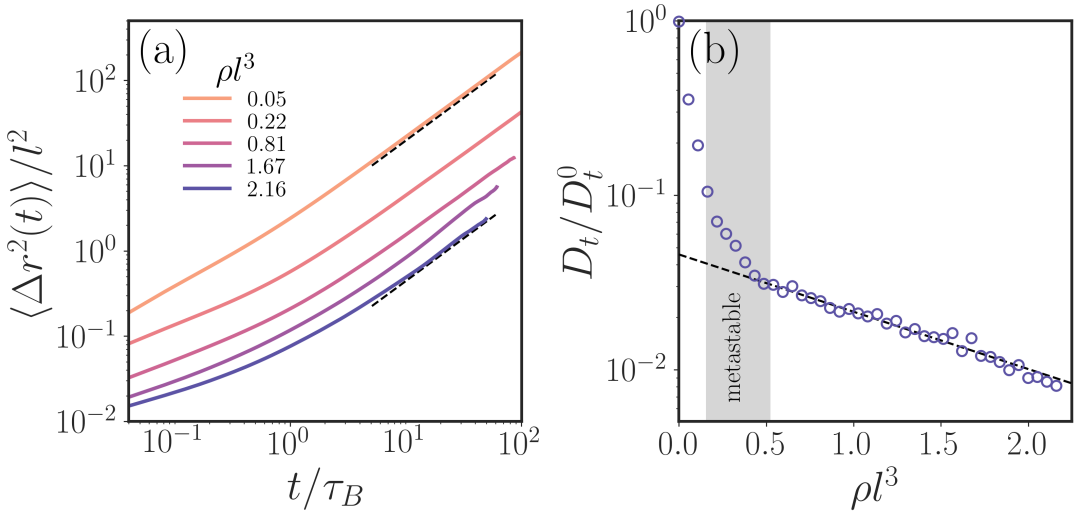

Supplementary FIG. 5: **Slowdown of translational motion in Brownian dynamics simulations**. The interaction strength is $\beta\Gamma = 67$. (a) Mean squared displacement $\langle \Delta r^2(t) \rangle$ at different number densities ρ. Black dashed lines indicate the regime were the long-term translational dynamics are diffusive again, i.e. $\langle \Delta r^2(t) \rangle \sim t$. (b) The long-time translational diffusion coefficient D_t as a function of the number density ρ, showing an exponential slowdown of translational diffusion.

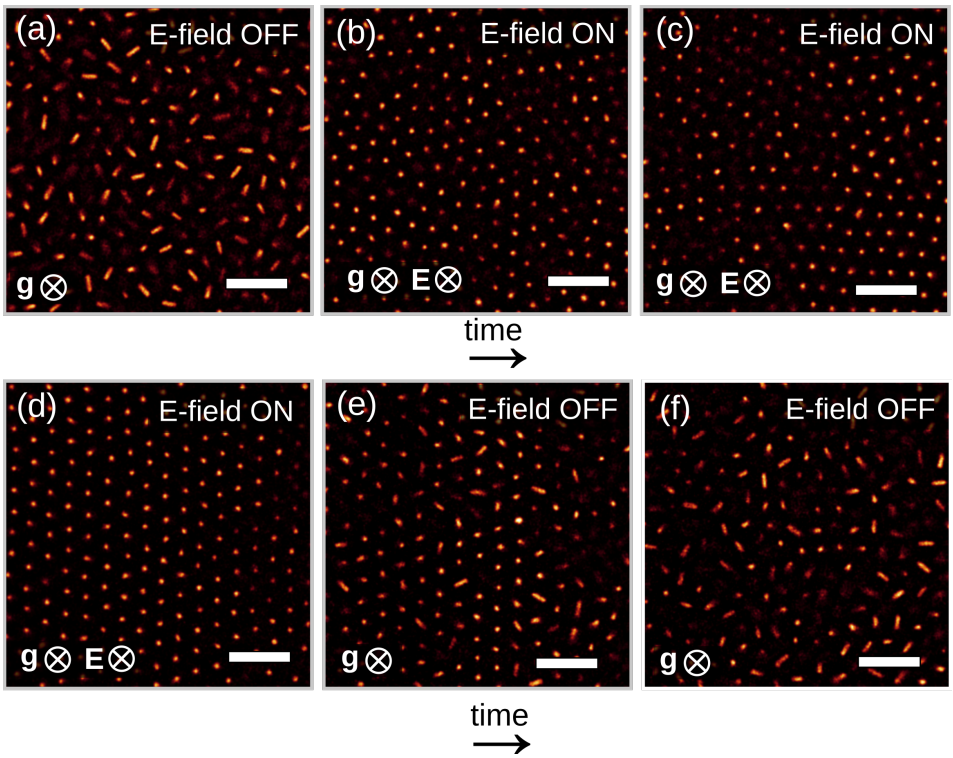

Supplementary FIG. 6: **Reversible switching between a plastic glass-forming phase and a crystal.** (a) Particles rotated, though they were positionally 'caged' without any long-ranged positional order. (b) Directly after application of an AC electric field ($E = 90$ V/mm, turned on by hand in ~ 5 s), particles aligned with the field. (c) Ordered clusters were formed that grew larger in time. (d) After 40 min the sample was fully crystalline. (e) Directly after the field had been turned off, an intermediate plastic crystal-like phase was observed. (f) After ~ 2 min, the long-ranged positional order was lost, particle orientations became random and the particles remained positionally caged. All scale-bars are 10 μm.

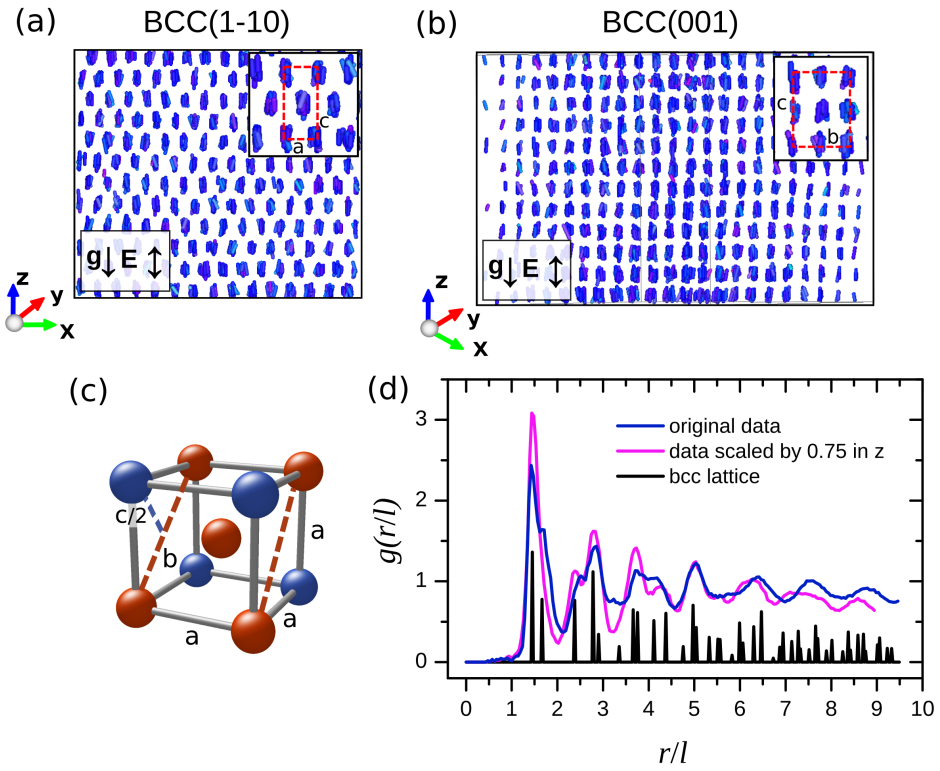

Supplementary FIG. 7: **Static 3D structure of the crystalline phase.** (a-b) 3D reconstruction of a crystalline phase, obtained from 3D confocal microscopy data analysis. Particles are color-coded according to their orientation. The crystalline phase formed under application of an electric field $E = 90$ V/mm. The particles formed a stretched body centered cubic (BCC) phase. (a) The view from the BCC(1-10) plane. (b) View from the BCC(001) plane shows that there is a significant elongation in the field (z) direction. For a perfect BCC lattice $b = c$ (see inset). (c) BCC unit cell, with the BCC(110) plane indicated with red spheres. (d) 3D radial distribution functions $g(r/l)$, with the end-to-end length of the particle $l = 2.29$ μm. The original data of the crystal are shown in red and the same data with all z-coordinates scaled by 0.75 in blue.

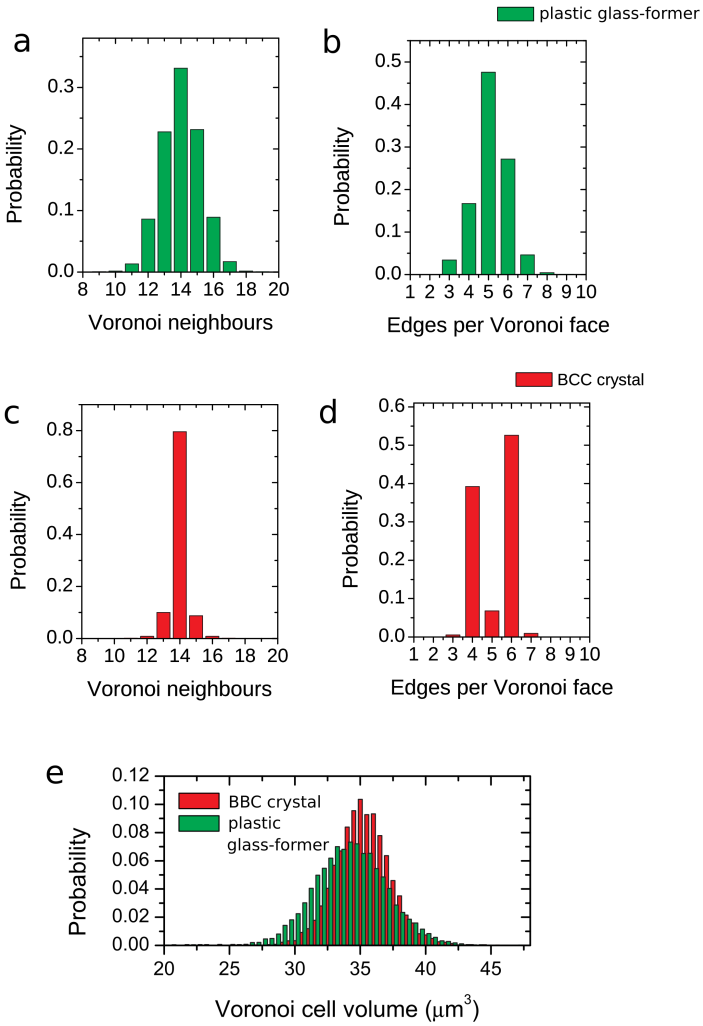

Supplementary FIG. 8: **3D Voronoi cell analysis**. (a-b) The Voronoi cells of particles in the plastic glassy phase had on average 14 Voronoi neighbours and Voronoi faces with on average 5 edges. (c-d) The number of neighbours of the particles in the crystal phase, formed after an external electric field was applied, is strongly peaked at 14 and the number of edges peaked at 4 and 6, which is in correspondence with the Voronoi cell of a perfect BCC crystal, i.e. a truncated octahedron. (e) Distribution of the Voronoi cell volume, which is inversely proportional to the local particle volume fraction. Using the hard-core particle dimensions, these values correspond to a volume fraction of approximately $\phi = 0.017$.